

Foraging energetics and prey density requirements of western North Atlantic blue whales in the Estuary and Gulf of St. Lawrence, Canada

Marie Guilpin^{1,2,*}, Véronique Lesage¹, Ian McQuinn¹, Jeremy A. Goldbogen³, Jean Potvin⁴, Tiphaine Jeanniard-du-Dot¹, Thomas Doniol-Valcroze⁵, Robert Michaud⁶, Michel Moisan⁶, Gesche Winkler²

¹Maurice Lamontagne Institute, Fisheries and Oceans Canada, 850 route de la Mer, Mont-Joli, QC G5H 3Z4, Canada

²Marine Science Institute, Quebec-Ocean — University of Quebec in Rimouski, 310 Allée des Ursulines, Rimouski, QC G5L 3A, Canada

³Department of Biology, Hopkins Marine Station, Stanford University, Pacific Grove, CA 93950, USA

⁴Department of Physics, Saint Louis University, 3450 Lindell Boulevard, Saint Louis, MO 63103, USA

⁵Pacific Biological Station, Fisheries and Oceans Canada, 3190 Hammond Bay Rd, Nanaimo, BC V9T 6N7, Canada

⁶Group of Research and Education on Marine Mammals, 108 de la Cale Sèche, Tadoussac, QC G0T 2A0, Canada

ABSTRACT: Foraging efficiency (FE) is determined by the ratio of energy intake to energy expenditure and represents a metric for estimating the capacity to store energy. Blue whales *Balaenoptera musculus* rely mostly on stored energy reserves for reproduction. They feed almost exclusively on krill, which vary in density and abundance both spatially and temporally. We used 10 depth–velocity archival tags deployed on blue whales foraging in the St. Lawrence Estuary, Canada, to identify feeding events. We modeled krill densities required to equal or exceed energy expenditures and allow energy storage. During the daytime, blue whales generally dove deeper and performed fewer but longer feeding dives than at other times of the diel cycle (10 vs. 28 feeding dives h⁻¹); however, they performed more lunges per dive during daytime (3 vs. 1 lunge dive⁻¹), which resulted in a stable feeding rate around the clock. Only 11.7 and 5.5 % of the Arctic and northern krill patches measured *in situ* contained densities allowing blue whales to achieve neutral energetic balance (FE = 1); less than 1.5 % of patches allowed FE of ≥3. While FE leading to successful reproduction and adequate fitness is unknown, these results underscore the necessity for blue whales to seek the highest densities within patches to reach neutral balance or allow energy storage. These findings further our understanding of blue whale foraging ecology and habitat suitability, and may help predict the effects of climate and natural variability or of potential fisheries on krill densities and blue whale condition.

KEY WORDS: Blue whale · *Balaenoptera musculus* · Energetics · Foraging efficiency · Krill density · Prey requirements · Foraging

Resale or republication not permitted without written consent of the publisher

1. INTRODUCTION

Marine predators face many obstacles to forage effectively in an environment where food resources most often exhibit a patchy, heterogeneous distribu-

tion in 3 dimensions. Diving mammals and birds have the additional constraint of having to regularly return to the water surface to replenish oxygen stores and remove metabolic by-products. They can therefore be considered central-place foragers with the

*Corresponding author: marieguilpin@gmail.com

surface as their essential return point (Houston 1985, Houston & McNamara 1985). Since they usually feed at depth, they allocate a significant amount of time and energy transiting to and from the surface, and have to factor this into their foraging decision process (Hoskins & Arnould 2013). A key assumption of the marginal value theorem is that, for a given time spent in a food patch, a predator requires access to higher prey densities when the patch is located further from its central point to offset the greater energy costs of reaching a more distant patch (MacArthur & Pianka 1966, Charnov 1976, Piatt & Methven 1992, Sparling et al. 2007). Central-place foragers should adjust their foraging effort using information acquired while foraging to select strategies that will maximize the energy gained per unit of energy expended (Caraco 1980, Rosenberg & McKelvey 1999). This capacity to modulate foraging time, or number of feeding events, with feeding depth or distance from the water surface or colony, has been shown in diving seabirds, pinnipeds, and cetaceans (Boyd 1996, Doniol-Valcroze et al. 2011, Ware et al. 2011, Watanabe et al. 2014).

In large free-ranging species, it is often difficult to calculate energy expenditure directly, especially since animals routinely engage in a multitude of activities in which each differs in energetic costs (Jeanniard-du-Dot et al. 2017a). However, isotopic (doubly-labeled water) or respiratory frequency approaches and, more recently, methods based on acceleration data from biologging devices have enabled estimating energy expenditure in a wide range of large species in relation to their foraging effort (Arnould et al. 1996, Fahlman et al. 2016, Ware et al. 2016). Energy expenditures measured in this way provide a basis as to how much energy animals need to extract from their environment when feeding to at least balance their metabolic costs. Given these metabolic rates, foraging efficiency (FE), i.e. the ratio between energy gain and energy expenditure, is expected to change with prey encounter rate and density (MacArthur & Pianka 1966): the higher the prey encounter rate or prey density, the greater the FE. Consequently, FE determines the energy available for the different life-history costs, influencing, for example, reproductive success and by extension population fitness (Costa 1993, Braithwaite et al. 2015, Jeanniard-du-Dot et al. 2017b, 2018). At $FE = 1$, i.e. the critical prey density threshold, the energy gained balances the energy spent with no energy surplus accumulation. This means that animals are capable of supporting their own growth and maintenance costs, but it is then unlikely that they would

have enough energy surplus to allocate to reproduction (Houston et al. 2007).

Marine mammals vary in life-history traits, reproduction strategies, and capacity for energy acquisition and storage (Costa 1993, Lockyer 2007). Income breeders need to forage throughout the breeding and nursing periods to provision their offspring adequately. Capital breeders fuel these life functions exclusively through endogenous reserves acquired and assimilated prior to breeding (Jonsson 1997, Madsen & Shine 1999, Houston et al. 2007, Wheatley et al. 2008). This means that species on the capital breeding end of the continuum of reproductive strategies rely on sufficient food supplies and resources to store the required fat reserves to maintain their basal body requirements, grow, and fuel reproduction (Brodie 1975, Costa 1993, Lockyer 2007). Poor body condition, when resources are scarce or when the environment is less profitable, lead to low female reproductive success in a number of marine mammal species (Arnould et al. 1996, Braithwaite et al. 2015, Seyboth et al. 2016, Jeanniard-du-Dot et al. 2017b). The capacity to accumulate energy is thus determinant for successful pregnancy and offspring survival, i.e. for individual fitness (Emlen 1966, Pyke et al. 1977), and therefore for population dynamics. In circumstances where the availability of high-quality food resources is ephemeral or limited to a short time window, predators are expected to adopt strategies that maximize FE and accumulation of surplus energy (Thompson et al. 1993, Jonsson 1997).

Blue whales *Balaenoptera musculus* are considered capital breeders, as they tend to acquire the critical energy reserves necessary for winter breeding and calving during the summer foraging period (Schoenherr 1991, Mate et al. 1999, Lesage et al. 2017). However, they may not fully fit this classical depiction of the annual cycle of capital breeders, as blue whales may take advantage of locally favorable feeding conditions when migrating (Bailey et al. 2009, Silva et al. 2013, Lesage et al. 2017). They are air-breathing mammals and thus central-place foragers that feed almost exclusively on aggregations of krill (Euphausiacea) (Kawamura 1980). Krill are heterogeneously distributed both in time and space, such that high-density patches at small scales (tens of km^2) are nested within low-density patches at larger scales (thousands of km^2) (Watkins & Murray 1998, McQuinn et al. 2015, 2016). These rapidly changing prey fields require that bulk filter feeders such as blue whales adopt foraging strategies that maximize FE under various scenarios (Goldbogen et al. 2015). A study of the mechanics, hydrodynamics, and ener-

getics of foraging blue whales suggests that they need to target extremely high-density krill patches to forage efficiently (Goldbogen et al. 2011). When they do, they can attain significantly higher FEs than other marine mammals, regardless of prey patch depth (Goldbogen et al. 2011). Blue whales have also been shown to adapt to the variability in prey depth and density by modulating their feeding rate and fine-scale maneuvers (Goldbogen et al. 2015). In the St. Lawrence Estuary in Canada, for instance, blue whales increased foraging time and number of feeding events as feeding depth increased, and fed nearer to the water surface when possible to reduce transit time, following the rules of optimal foraging (Doniol-Valcroze et al. 2011).

The western North Atlantic blue whale population is estimated to be in the low hundreds (Sears & Calambokidis 2002), and there are concerns that the calving rate might be low in this population (Beauchamp et al. 2009, C. Ramp unpubl. data). A low calving rate could be an indication of poor nutritional state and an incapacity for individuals to accumulate enough energy to carry a pregnancy to term. The Estuary and Gulf of St. Lawrence (EGSL) encompasses important summer feeding habitats for western North Atlantic blue whales. In this region, their diet consists on average of 70% Arctic krill *Thysanoessa raschii* and 30% northern krill *Meganycitiphanes norvegica* (Gavrillchuk et al. 2014). These 2 species vary in patch density, preferred water temperature, and depth of aggregation, as well as energy content (Plourde et al. 2014, McQuinn et al. 2015, Cabrol et al. 2019). Consequently, choosing one or the other will likely affect blue whale foraging energetics and efficiency. Hence, this can impact their capacity to accumulate energy stores to successfully reproduce and survive, and ultimately their population dynamics. The western North Atlantic blue whale population has been listed as 'endangered' under the Canadian Species at Risk Act since 2002. Therefore, there is a pressing need to better understand the prey densities that blue whales require not only to maintain homeostasis, but also to accumulate energy for reproduction or other purposes.

The objective of this study was to estimate the krill densities required by blue whales in their environment to meet or exceed energy demands and achieve $FE \geq 1$. We first determined energy requirements of the blue whales using depth-specific foraging effort obtained from archival tag data of previous studies (Doniol-Valcroze et al. 2011, 2012) along with parameters from mechanistic and bio-energetic models

(Goldbogen et al. 2011, Potvin et al. 2012). Given these energy expenditures and measurements of krill energy content, we then estimated the krill densities required for different FE scenarios. Lastly, we compared these krill densities to *in situ* acoustically measured krill densities to assess the range of FEs blue whales are likely to reach in this region when feeding on Arctic krill or northern krill. Results will improve our understanding of habitat and prey requirements for these animals and provide insights into potential effects of a warming climate on the quality of one of their main feeding habitats in the western North Atlantic.

2. MATERIALS AND METHODS

2.1. Tag data and foraging effort

Nine velocity-time-depth recorders (VTDRs Mk8; Wildlife Computers) and 1 digital acoustic recording tag (D-tag; Johnson & Tyack 2003), along with radio-transmitters, were deployed on blues whales in the St. Lawrence Estuary (SLE, Quebec, Canada, 48° 18' N, 69° 20' W) during August and September of 2002 to 2009. Tags were temporarily attached to whales with suction cups, and deployed from a 5 m rigid-hulled inflatable boat using a hand-held pole or a crossbow. A high-power directional VHF antenna and multiple observers allowed tracking of the whales from a distance (500–1000 m) to minimize boat disturbance. Tagged whales were tracked until nightfall or until tag detachment through the corrosion of a magnesium cap as a suction release system (Doniol-Valcroze et al. 2011, 2012). The swim velocity (measured from a pressure transducer resolution of 0.25 m), diving depth, and water temperature were sampled every second (1 Hz). Estimates of swim speed for the D-tag were obtained from flow noise data (sampling rate 1 Hz) following Goldbogen et al. (2008).

A dive was defined as a vertical excursion below 0.25 m (Doniol-Valcroze et al. 2011, 2012). Lunges or feeding events and depths at which they occurred were identified from swimming speed patterns alone using a robust technique developed by Doniol-Valcroze et al. (2011). This algorithm exploits the abrupt changes in swim speed, characteristic of lunge feeding, occurring during the acceleration phase and subsequent mouth opening (Croll et al. 2001, Goldbogen et al. 2006). Dives including at least 1 feeding attempt were labeled 'feeding dives.' Dives with no feeding events were considered 'non-feeding dives' and included non-foraging behaviors (e.g.

traveling or resting dives), surface breathing, and exploratory dives. Other parameters were also extracted from the dive data, including dive duration and maximum depth, as well as the number of lunges and depths at which they occurred, i.e. depth at which mouth opening was maximum and marked by a sharp decrease in swim speed, for feeding dives.

Given that energetic costs vary between ascending, descending, and lunge feeding, dives were separated into more energetically homogeneous segments. For feeding dives, descent was the period between the start of a dive (i.e. below 0.25 m depth) and the first lunge; ascent was the period following the last lunge but prior to reaching the surface. Transit was the combination of both descent and ascent. Foraging time corresponded to the period between the start of the first lunge and end of the last lunge within a dive. For non-feeding dives, the period when animals remained within 80 and 100% of their maximum dive depth corresponded to the bottom phase. Descent and ascent preceded and followed this phase.

Foraging effort was examined on an hourly basis and was described in terms of feeding depth, dive duration, and feeding rate. The latter was expressed as the number of lunges h^{-1} , number of feeding dives h^{-1} , and number of lunges $\text{dive}^{-1} \text{h}^{-1}$. We used general additive mixed models (GAMMs) in the 'mgcv' package (Wood 2006) in R (v3.3.3; R Development Core Team 2017) to investigate hourly variability in 5 response variables: feeding depth, dive duration, and 3 feeding rate indices, i.e. number of lunges h^{-1} , number of feeding dives h^{-1} , and number of lunges $\text{dive}^{-1} \text{h}^{-1}$. Hour of the day, the only covariate included in the model, was incorporated as a smoothed term using cyclic cubic regression splines ($k = 24$, or 1 h^{-1}) and modeled against each of the 5 response variables in separate GAMMs. Individual whales were set as a random effect. Sex was not included as an explanatory variable, as it was unknown for 2 of the 10 tagged whales; including this variable would have resulted in a reduction of an already small sample size. Interannual variations in diving patterns were also not investigated given that only 1 blue whale was tagged per year except in 2004 (4 tagged whales). We assessed the significance of covariates using a likelihood ratio test comparing each model against the null model which included only the random effect. We assessed homogeneity of variances in the models from plots of residuals versus fitted values, and normality of the residuals using quantile-quantile plots and residual histograms. Hourly mean foraging effort was compared among periods of the

day using either a Student's *t*-test or a Mann-Whitney *U*-test, depending on normality of the data. Periods of the day were date-specific to account for variations in sunrise and sunset times during the study period. Daytime strictly included daylight hours; dusk and dawn were defined by the nautical twilight times; night included hours after sunset and before sunrise. We pooled dusk, dawn, and night hours together (referred to as 'nighttime hours' hereafter) for comparison against daytime hours.

2.2. Energy expenditure

Accurate estimates of gross energy expenditure require activity-specific metabolic rates (Jeanniard-Dot et al. 2017a). These parameters are difficult to measure in free-ranging cetaceans, especially large-sized species such as blue whales. In these species, mass-specific basal metabolic rate (BMR, in J s^{-1}) and active metabolic rate (AMR, in J s^{-1}) have been calculated by scaling values obtained from terrestrial animals and smaller marine mammals (Kleiber 1975, Croll et al. 2001). Recently, Goldbogen et al. (2006) and Potvin et al. (2012) used hydrodynamic and mechanistic models to predict AMR for rorquals. They defined the lunge/filter metabolic rate (hereafter LFMR, in J s^{-1}), which takes into account the extra power required to overcome the drag created by the expanded ventral pouch during the engulfment phase of lunge feeding. Mass-specific BMR, where M represents body mass in kg, was obtained following Kleiber (1975), whereas AMR and LFMR were based on scaled equations of Potvin et al. (2012):

$$\text{BMR} = 2 \times (4 \times M^{0.75}) \quad (1)$$

$$\text{AMR} = 3 \times \text{BMR} \quad (2)$$

$$\text{LFMR} = 1.6 \times \text{AMR} \quad (3)$$

We modeled energy expenditure for each dive, and separately for each dive type (feeding or non-feeding) and dive phase (descent, ascent, bottom, and foraging in the case of foraging dives). Blue whale foraging dives typically consist of a descent where passive gliding occurs on average 40% of the time, one or multiple lunges at depth, and an ascent powered by steady swimming (Goldbogen et al. 2011). Gliding is a key energy-saving strategy for diving marine mammals, the use of which depends on maximum dive depth, dive duration, and body condition of the animals (Williams et al. 2000, Miller et al. 2012, Narazaki et al. 2018) and thus is also expected to

occur in non-feeding dives. A study of diving cost-efficiency indicates that blue whales are negatively buoyant and start gliding at depths of approximately 18 m from the surface when diving at depths of 36 to 88 m (Williams et al. 2000). In our analysis, we considered this strategy as being part of the descent phase for both foraging and non-foraging dives with maximum depths exceeding 18 m. Accordingly, the energy expenditure of non-feeding dives (in kJ) at depths of 18 m or more was calculated as follows:

$$\begin{aligned} \text{Energy expenditure}_{(\text{non-feeding dive} > 18 \text{ m})} = & \\ & (0.60 \text{ Descent time} \times \text{AMR} + \\ & 0.40 \text{ Descent time} \times \text{BMR} + \\ & \text{Bottom time} \times \text{AMR} + \\ & \text{Ascent time} \times \text{AMR}) / 1000 \end{aligned} \quad (4)$$

The energy expenditure of non-feeding dives (in kJ) shallower than or equal to 18 m was calculated based on total dive duration as follows:

$$\text{Energy expenditure}_{(\text{non-feeding dive} \leq 18 \text{ m})} = (\text{Dive time} \times \text{AMR}) / 1000 \quad (5)$$

The energy expenditure of feeding dives (in kJ) was calculated similarly as for non-feeding dives deeper than 18 m, while accounting for extra costs during the foraging phase:

$$\begin{aligned} \text{Energy expenditure}_{(\text{feeding dive} > 18 \text{ m})} = & \\ & (0.60 \text{ Descent time} \times \text{AMR} + \\ & 0.40 \text{ Descent time} \times \text{BMR} + \\ & \text{Foraging time} \times \text{LFMR} + \\ & \text{Ascent time} \times \text{AMR}) / 1000 \end{aligned} \quad (6)$$

The energy expenditure of feeding dives (in kJ) shallower than or equal to 18 m was calculated in a similar way as for feeding dives deeper than 18 m, except without taking gliding into consideration:

$$\begin{aligned} \text{Energy expenditure}_{(\text{feeding dive} \leq 18 \text{ m})} = & \\ & (\text{Descent time} \times \text{AMR} + \text{Foraging time} \times \\ & \text{LFMR} + \text{Ascent time} \times \text{AMR}) / 1000 \end{aligned} \quad (7)$$

Potvin et al. (2012) calculated specific metabolic rates for different phases of a lunge (prey approach, engulfment, filtering) through biomechanical and hydrodynamic modeling. Engulfment is the costliest part of a lunge but only accounts for approximately 6% of the total lunge duration; the prey approach/filterer metabolic rates and LFMR are of the same order of magnitude. The limited number of tag sensors prevented us from obtaining the kinematic details

needed to apply specific metabolic rate to filtration, engulfment, and prey approach times. The application of LFMR to the entire foraging time during a dive was a reasonable assumption when calculating foraging costs over extended periods of time that included multiple lunges and dives, as it balanced the overestimated costs of filtering with the underestimated costs of lunging. To reflect changes in metabolic rate with body size, energy expenditure was calculated for 3 body lengths, i.e. 22, 25 and 27 m. These values reflect the size of sexually mature blue whales from the northern hemisphere (21–23 m for females, approximately 22 m for males; Sears & Calambokidis 2002), and are within the range of the maximum of 27 m documented for the North West Atlantic Ocean (Sears & Perrin 2009).

The relationship between energy expenditure and dive duration, maximum dive depth, and number of lunges was examined using linear mixed effects (LME) models in the ‘nlme’ package in R (Pinheiro et al. 2013) and checked for model assumptions, with individual whales as a random effect. We examined potential temporal variation in hourly energy expenditure with GAMMs, using the approach and validation process described previously.

2.3. Krill density requirements

Depth-specific foraging effort and linked energy expenditure while foraging in the SLE were used to estimate the krill densities required by blue whales to meet or exceed energy demands and thus build energy reserves. A key assumption of our approach is that the foraging effort observed in the 10 tagged individuals is assumed to represent the best strategies chosen by the animals and adapted to the foraging conditions for that depth and time of day. We estimated krill density requirements (g wet weight m⁻³; hereafter, all weights indicated are wet weights, unless otherwise noted) for i , the i^{th} hour, using energy expenditure (from Eqs. 4–7), and a set of fixed FEs (i.e. 1, 2, 3, 4):

Krill density _{i} =

$$\frac{\text{Foraging efficiency} \times \text{Energy expenditure}_i}{\text{VE} \times \text{Feeding rate}_i \times \text{KEC} \times \text{AE} \times \text{SR}} \quad (8)$$

where VE is the volume of engulfment (in m³), feeding rate is estimated by the number of lunges h⁻¹, KEC is the krill energy content (kJ g⁻¹), AE is the assimilation efficiency, and SR is success rate (see Table 1 for specific values). An FE of 1 indicates a

Table 1. Input parameters, associated sampling distributions and/or values (mean \pm SD where applicable) and data sources for estimating blue whale krill density requirements. na: not applicable

Parameter	Description (units)	Value	Distribution	Source
FE	Foraging efficiency	1, 2, 3, 4	Fixed parameter	
Energy expenditure _{<i>i</i>}	Size-specific energy expended	Hour-specific	Gamma	Tag data, this study
Feeding rate _{<i>i</i>}	Number of lunges h ⁻¹	Hour-specific	Gamma	Tag data, this study
VE	Length (<i>L</i>)-specific engulfment volume (m ³)	(1.023 × <i>L</i> ^{3.65}) / 1025	na	Goldbogen et al. (2010)
<i>M</i>	Length-specific body mass (kg)	61318 (22 m), 96568 (25 m), 122605 (27 m)	na	Croll et al. (2001)
KEC _{tr}	Krill energy content (kJ g ⁻¹ wet weight) <i>Thysanoessa raschii</i>	4.3 ± 0.58	Normal	D. Chabot (unpubl. data), V. Lesage (unpubl. data)
KEC _{mn}	Krill energy content (kJ g ⁻¹ wet weight) <i>Meganyctiphanes norvegica</i>	5.2 ± 0.45	Normal	D. Chabot (unpubl. data), V. Lesage (unpubl. data)
AE	Assimilation efficiency	0.84–0.93	Uniform	Goldbogen et al. (2011), Olsen et al. (2000), Mårtensson et al. (1994)
SR	Success rate	1	Fixed	

neutral balance between gross energy intake and expenditure, and represents the theoretical krill density threshold below which foraging is no longer beneficial. Efficiencies above 1 indicate a capacity to build energy reserves. We used the FE ratio, i.e. the ratio between energy intake and energy expenditure, for each time bin (*i*) of 1 h as the starting point of our estimations (Goldbogen et al. 2011):

$$\text{Foraging efficiency}_i = \frac{\text{Energy intake}_i}{\text{Energy expenditure}_i} \quad (9)$$

We calculated energy expenditure (kJ) from the dive data using the procedure outlined above. Energy intake (in kJ) needed to be estimated using information on a number of variables, including the number of lunges h⁻¹ (feeding rate), volume of engulfment in m³ (VE), krill density in g m⁻³, krill energy content in kJ g⁻¹ (KEC), the assimilation efficiency (AE), and success rate (SR) using the following equation (Goldbogen et al. 2011):

$$\text{Energy intake}_i = \text{VE} \times \text{Feeding rate}_i \times \text{Krill density} \times \text{KEC} \times \text{AE} \times \text{SR} \quad (10)$$

Krill densities estimated in Eq. (5) represented the density required to cover the cost of any feeding and non-feeding dives performed during each 1 h time bin *i* (i.e. FE = 1) or the density required to cover these costs and to store surplus energy (i.e. FE > 1). We ran Monte Carlo simulations to estimate krill density requirements while incorporating uncer-

tainty of input parameters. Uncertainties around each input parameter were either data-driven or taken from the literature, and were described with sampling distributions that best captured the inherent variability associated with biological data (Table 1). Parameter values were randomly drawn from their assigned distributions in each model iteration. Sets of 10 000 iterations were run for each of the defined FEs, for each whale length, and for each hour of the day to obtain a mean, standard deviation (SD), and a 90 % confidence interval (CI) around estimated krill density requirements.

Energy expenditure h⁻¹ and feeding rate (number of lunges h⁻¹) were fitted with gamma distributions for each hour of the day. A gamma distribution is well suited for highly variable, continuous, and strictly positive data. However, the gamma distribution of feeding rates needed to be constrained between 1 lunge and a maximum of 60 lunges h⁻¹ for physiological consistency, since a lunge lasts between 60 and 98 s (Goldbogen et al. 2006, 2008, 2011, Potvin et al. 2012). The upper bound of the gamma distribution of energy expenditure was constrained to a cost equivalent to 60 lunges. Distributions for both parameters were defined by shape and scale parameters, which were parameterized from the mean and SD with shape = mean²/SD² and scale = SD²/mean. Engulfment volume is allometric to body length (Potvin et al. 2010, Goldbogen et al. 2012) and was calculated for the 3 selected body lengths following Goldbogen et al. (2010) (Table 1).

AE was assumed to be uniformly distributed from 0.84 to 0.93 (Table 1). The AE of 0.84 from Lockyer (1981, 2007) has been commonly used in studies on rorqual FE (Goldbogen et al. 2011). The highest value (0.93) was based on digestive efficiency documented for krill in minke whales *Balaenoptera acutorostrata* (Mårtensson et al. 1994).

Arctic krill *Thysanoessa raschii* and to a lesser extent *T. inermis* represent up to 70% of blue whale diet in the EGSL, the rest being northern krill *Meganyctiphanes norvegica* (Gavrilchuk et al. 2014). Arctic krill are generally found higher in the water column and form denser patches than northern krill in this ecosystem (McQuinn et al. 2015). Krill density requirements were modeled assuming a 100% diet of either Arctic or northern krill. Species-specific energy content was obtained by bomb calorimetry (kJ g^{-1}) (Phillipson 1964) using krill sampled in the EGSL during the blue whale feeding period, i.e. from May to September. A normal distribution was fitted to the data to represent all krill body lengths, life stages, and seasonal changes of lipid content (Table 1).

Prey capture success rate is difficult to measure in free-ranging animals, and has yet to be measured for bulk filter feeders like rorquals. The feeding techniques exhibited by blue whales suggest a high degree of specialization to maximize prey capture and minimize the escape of individual krill. For example, the rolling behavior of blue whales (Goldbogen et al. 2012) is thought to be a way of anticipating the escape response of krill (Potvin et al. 2012) and maximizing prey capture. Considering the speed at which a whale lunges (Potvin et al. 2010) and documented feeding maneuvers (Goldbogen et al. 2013, Cade et al. 2016), krill escapement was assumed negligible and therefore krill capture success rate was assumed to be 1.

We assessed hourly variations of krill density requirements using a generalized additive model (GAM) in the 'mgcv' package in R (Wood 2006). Cyclic cubic regression splines were applied to the temporal variable, i.e. hour of the day. Model selection was done using a likelihood ratio test comparing our model against the null model. Equal variance and normality of the residuals were assessed through scatter plots of residuals versus fitted values, quantile-quantile plots, and residual histograms. Model sensitivity to uncertainty in input parameters was explored for each parameter using a partial correlation coefficient sensitivity analysis and the 'pcc' function of the R package 'sensitivity' (Pujol et al. 2016). This method accounted for the correlation between feeding rate and energy expenditure. Data analysis was conduc-

ted under the R programming language (R Development Core Team 2017).

2.4. Preyscape: *in situ* krill densities

Hydroacoustic data were collected during surveys conducted between 2009 and 2015 in the EGSL (Quebec, Canada, 49° 43' N, 65° 11' W) (Table 2). Data were recorded during daytime using a calibrated (Demer et al. 2015) Simrad® EK60 multi-frequency echosounder (38, 70, 120, and 200 kHz). Systematic hydroacoustic sampling was performed whenever blue whales were present and repeatedly seen (but not tagged) by trained onboard marine mammal observers. Sampling was either in the form of a rectangular 'spiral' (concentric lines of increasing distance and length from the center starting point; see Fig. S1a in the Supplement at www.int-res.com/articles/suppl/m625p205_supp.pdf) or a 'grid' (parallel equidistant lines; Fig. S1b) of ~0.5 km spacing grid size. Both designs, totaling 8 to 128 km² of sampled area, provided adequate spatial resolution to characterize the krill patches.

Hydroacoustic data were edited to remove non-biological echoes and noise from the surface to the seabed reflection. We echo-integrated data into high-definition bins of 3 pings on the horizontal axis by 0.5 m depth on the vertical axis. Acoustic classification of prey was done using species-specific multi-frequency algorithms developed for the western GSL (McQuinn et al. 2013). Biological echoes were classified between the 2 species of krill, namely Arctic and northern krill.

Table 2. Summary of 'grids' and 'spirals' (see Fig. S1 in the Supplement) from hydroacoustic surveys used for krill patch characterization. GSL: Gulf of St. Lawrence; SLE: St. Lawrence Estuary

Survey	Location	Year	Type	Area covered (km ²)	Number of lines
C1522	GSL	2015	Grid	16	6
			Spiral	14	7
C1410	GSL	2014	Grid	24	4
C1223	GSL	2012	Spiral	8	3
			Spiral	38	3
			Grid	60	5
C0962	SLE	2009	Grid	16	3
			Grid	64	6
			Grid	126	6
			Grid	128	10

We used the classified volume backscattering coefficient (S_v in $\text{m}^2 \text{m}^{-3}$) and its logarithmic form, mean volume backscattering strength (MVBS or S_v in dB re $1 \text{ m}^2 \text{m}^{-3}$) to infer species-specific krill density (g m^{-3}) for each echo-integrated bin. Krill biomass density was calculated using a weight-based target strength (TS_W) function:

$$\text{TS}_W = \text{TS}_N - 10\text{Log}(W) \quad (11)$$

where W is the mean wet weight (g) of an individual krill (i.e. 56.2 and 298 mg for Arctic and northern krill, respectively). TS_N is the length-based modeled target strength (McQuinn et al. 2013) for each species assuming average length, and TS_W is -70.0 and -69.0 dB g^{-1} for Arctic krill and northern krill, respectively. From this relationship, krill density (D_k) was calculated as:

$$D_k = S_v / 10^{(\text{TS}_W / 10)} \quad (12)$$

To account for the anisotropy of krill distribution in relation to the shoreline (Simard & Lavoie 1999, McQuinn et al. 2015), only transects perpendicular to the slope were used in the estimation of patch density and distribution. We used a threshold of 4 g m^{-3} to discriminate between weakly aggregated krill, which includes empty bin cells, and aggregated krill patches (McQuinn et al. 2015). For each grid or spiral sampled, the mean, maximum, minimum, and quantiles of krill densities (g m^{-3}) were used to describe the vertical distributions of bins containing aggregated Arctic and northern krill. For each patch, estimated *in situ* krill densities during daytime were compared to those modeled for the same period, while estimating the percentage of density bins that exceeded each FE threshold. This analysis allowed us to determine the likelihood of a blue whale finding and exploiting krill patches meeting the different FE thresholds, as well as the potential FE that a blue whale is likely to reach when foraging in the EGSL.

3. RESULTS

The 9 VTDR and the 1 D-Tag deployed on blue whales provided data for 2 to 25 h (average 13 h), and a total of 137 h. Tagging efforts were initiated early after sunrise but tags were often only successfully deployed later in the day. As a result, data were unevenly distributed during the day, with a larger coverage of the period between noon and sunset compared with early in the day (Fig. S2). Feeding dives ($N = 1718$) were recorded from all whales, although some variability in feeding activity was

noted among individuals. Whales performed on average (\pm SD) 172 ± 147 feeding dives and 271 ± 203 lunges during the tracking period, but these numbers varied from 9 to 390 feeding dives and from 40 to 576 lunges. Another 4115 dives corresponded to the shallow dives performed in-between surface breaths, i.e. inter-breath intervals (average per whale: 412 ± 331 ; range: 57–972), and 844 dives (average per whale: 85 ± 68 ; range: 3–196) corresponded to underwater behaviors other than feeding.

3.1. Hourly foraging effort and energy expenditure

Significant diel variations were detected in feeding depth, feeding dive duration, number of feeding dives h^{-1} , number of lunges dive^{-1} , and number of lunges h^{-1} (Fig. 1, Table 3). Generally, blue whales fed at deeper depths (Mann-Whitney $U = 143$, $p < 0.0001$) and performed longer dives during daytime compared to nighttime (including dusk, night and dawn, Mann-Whitney $U = 141$, $p < 0.0001$; Fig. 1, Table 4). Feeding dives were 2.5 times less frequent during daytime (Student's t -test, $df = 21$, $p < 0.0001$), but had 3 times more lunges than dives performed during nighttime (Student's t -test, $df = 21$, $p < 0.0001$). However, when examined on an hourly basis (thus including transit and surface times), feeding rate expressed as the number of lunges per hour was approximately 25% less during daytime compared to nighttime (Fig. 1).

Energy expenditure during feeding dives increased significantly (LMEs, all $p < 0.05$) with maximum dive depth, dive duration, and the number of lunges d^{-1} , but more rapidly as whale size increased (i.e. steeper slope for the relationship; Fig. 2). However, when examined on an hourly basis rather than a dive by dive basis, energy expenditure remained relatively unchanged throughout the day ($edf = 22$; $F = 0$, $p = 0.48$), with an average $455\,206 \pm 111\,604 \text{ kJ}$ expended during daytime hours vs. $456\,583 \pm 95\,112 \text{ kJ}$ during nighttime (Fig. 3).

3.2. Krill density requirements

Krill density requirements for feeding blue whales varied depending on time of day, but in a similar fashion when feeding on Arctic krill or northern krill (Fig. 4, Table 5). Density requirements tended to be higher in the early morning than at other times of day or night; this corresponded to the period when whales were diving

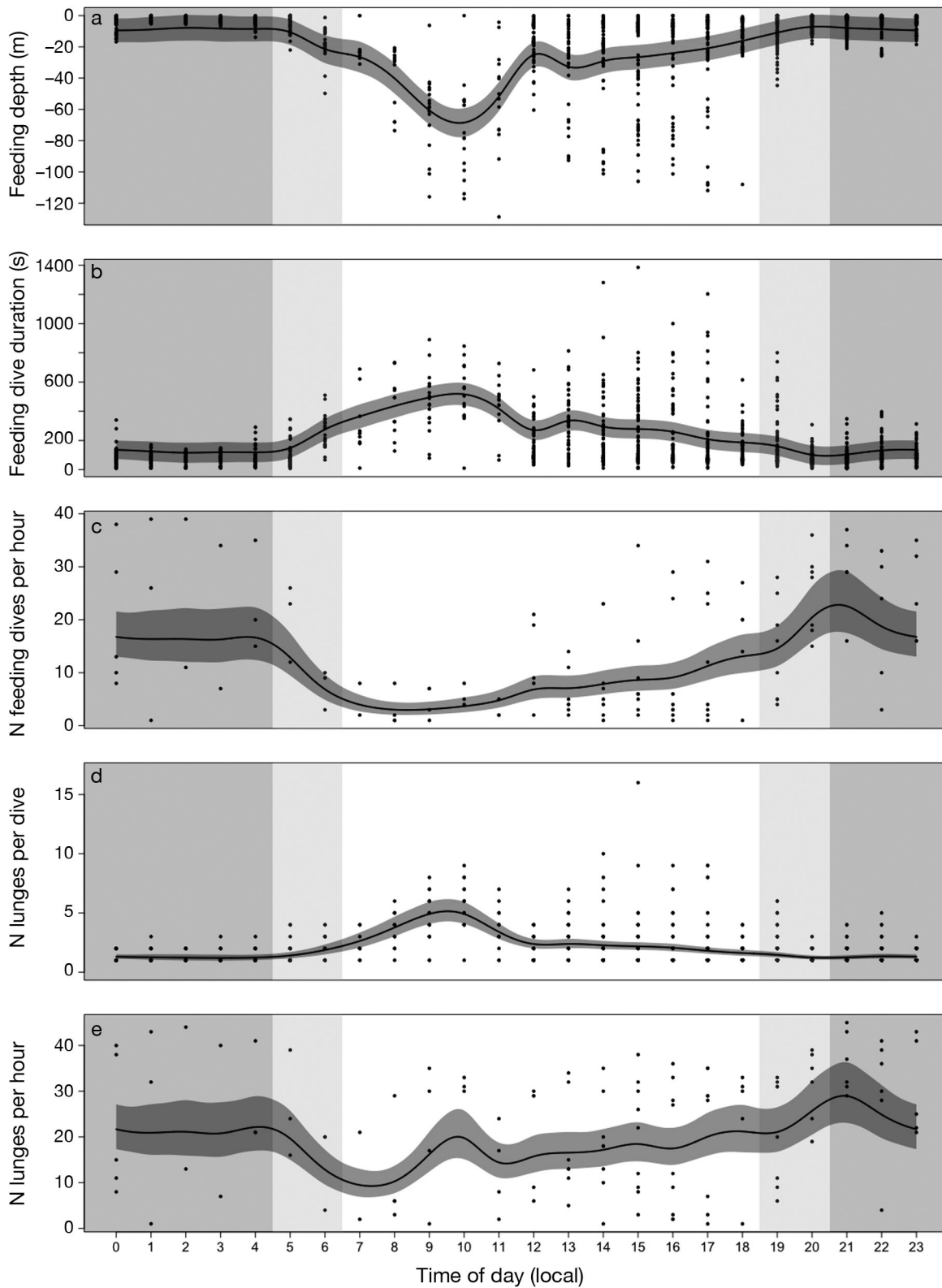


Fig. 1. Predicted change in blue whale foraging effort with time of day in (a) feeding depth (m), (b) dive duration (s), (c) number of feeding dives, (d) number of lunges d^{-1} , and (e) number of lunges h^{-1} . Dark grey ribbons represent the 95% confidence intervals around the predicted response from generalized additive mixed models. Shaded areas are for nighttime (grey), dusk and dawn (light grey), and daytime (white). Points are data observations. (See Table 3 for full statistical results)

Table 3. Trends in various indices of foraging effort with time of day, based on generalized additive mixed model (GAMM) results, and using individual blue whale as a random effect. Results (p-values) of the likelihood ratio test (LRT) for model selection against the null model (random effect only) are also presented; edf: estimated degrees of freedom

Response variable	N	Adjusted R ²	p	edf	F	LRT
Feeding depth (m)	1718	0.385	<0.001	18.3	44.4	<0.0001
Feeding dive duration (s)	1718	0.316	<0.001	16.9	34.9	<0.0001
Total number of feeding dives per hour	137	0.267	<0.001	12.8	19.7	<0.0001
Number of lunges per feeding dive	1718	0.282	<0.001	11.3	16.3	<0.0001
Total number of lunges per hour	137	0.087	<0.001	14.7	11.4	<0.0001

Table 4. Characteristics of feeding dives and feeding rates (mean ± SD) during daytime vs. nighttime. Nighttime includes dusk, night, and dawn. Statistical differences (Mann-Whitney *U*-test and Student's *t*-test) are indicated with an asterisk (*p < 0.05)

Parameter	Day	Night
Feeding depth (m)*	39.8 ± 19.6	4.9 ± 3.1
Feeding dive duration (s)*	371.9 ± 115.8	95.8 ± 44.8
No. of feeding dives h ⁻¹ *	9.9 ± 4.7	27.9 ± 4.2
No. of lunges per feeding dive*	3.1 ± 1.2	1.3 ± 0.2
No. of lunges h ⁻¹ *	23.2 ± 4.7	30.6 ± 4.1

deeper and for longer, and were performing a larger number of lunges dive⁻¹ (Figs. 1d & 5). Globally, krill densities that a 25 m blue whale required to balance energy expenditures were higher during daytime feeding than at night, and when feeding on Arctic krill rather than on northern krill (Mann-Whitney *U* = 50 085 × 10⁵ and 20 428 × 10⁶; both p < 0.0001; Figs. 4 & 5). Mean ± SD density requirements were 40.9 ± 49.8 g m⁻³ for Arctic krill and 33.3 ± 39.3 g m⁻³ for northern

krill, when feeding during daytime, compared to 31.7 ± 38.1 and 25.8 ± 31.0 g m⁻³, respectively, when feeding at nighttime (including night, dusk, and dawn; Fig. 5).

Krill densities need to be considerably higher in order for blue whales to reach higher FEs and accumulate reserves (Kruskal-Wallis test, df = 3, p < 0.0001; Fig. 5). For instance, median required Arctic krill densities, which varied for a 25 m whale from 14 to 40 g m⁻³ depending on time of day, would need to increase to 56–159 g m⁻³ for this whale to reach an FE of 4 (Fig. 5a). The predicted required krill density of northern krill for a 25 m blue whale to balance its energy expenditures (FE = 1) followed similar patterns as for Arctic krill, and ranged from a median of 11 to 33 g m⁻³ depending on time of day (Fig. 5b). To achieve an FE of 4, northern krill median densities would need to reach values ranging from 46 to 131 g m⁻³ depending on time of day (Fig. 5b). These results indicate that while krill density requirements varied similarly with FE among the 2 krill species, higher densities were required when feeding on

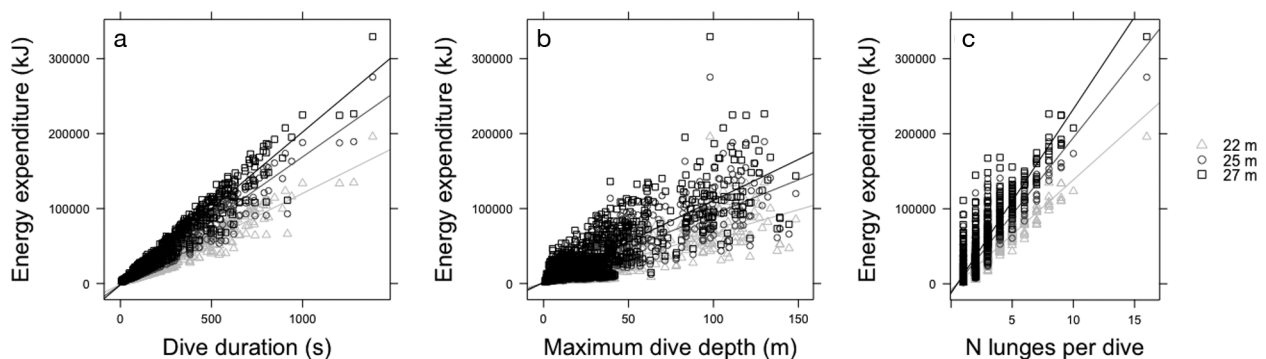


Fig. 2. Relationship between energy expenditure during feeding dives for 3 blue whale sizes (22, 25, and 27 m length) and (a) dive duration (s) (mean ± SE slope for 22 m: 122 ± 0.6; 25 m: 171 ± 0.9; 27 m: 205 ± 1), (b) maximum dive depth (m) (22 m: 650 ± 11; 25 m: 914 ± 15; 27 m: 1093 ± 19) and (c) number of lunges per dive (22 m: 14 265 ± 148; 25 m: 20 054 ± 210; 27 m: 23 986 ± 252). Relationships were modeled using linear mixed models (all p < 0.05)

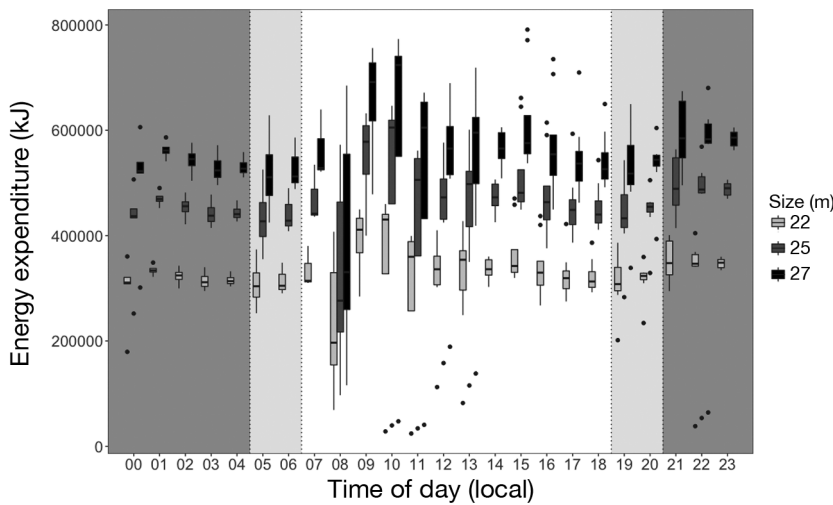


Fig. 3. Diel distribution of energy expenditure for a 22, 25, and 27 m blue whale. Box plots present the median (solid horizontal line), lower and upper quartiles (boxes), extreme values (whiskers) and outliers (points). Shaded areas are for nighttime (dark grey), dusk and dawn (light grey), and daytime (white). The large confidence interval at 08:00 h is a combination of natural variability among individuals in feeding effort and small sample size ($n = 4$)

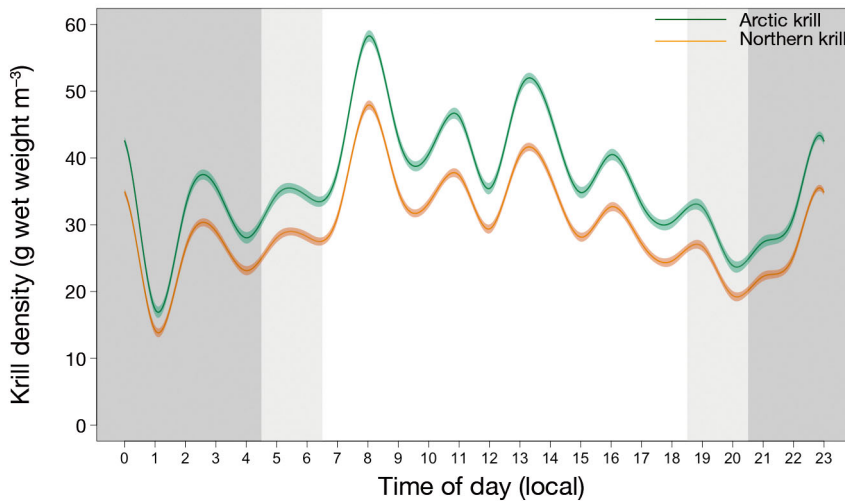


Fig. 4. Diel variation in the predicted response of estimated krill density required for a foraging efficiency of 1 by blue whales feeding on Arctic and northern krill. The y-axis represents the predicted response from generalized additive models on the mean krill density (solid line), including the 95% confidence intervals (ribbons). Shaded areas are for nighttime (dark grey), dusk and dawn (light grey), and daytime (white). (See Table 5 for full statistical results)

the smaller, and energetically less rewarding, Arctic krill than northern krill. Density requirements according to FE and krill species followed a similar pattern for a 22 or 27 m whale as for a 25 m whale, but were offset as a result of the positive allometric scaling of engulfment volume with whale size (Fig. S3).

The sensitivity analysis highlighted the feeding rate (number of lunges h^{-1}) and energy expenditure as the largest contributors to the uncertainty in predicted krill density requirements (Table 6).

3.3. *In situ* krill preyscape

Ten ‘spirals’ or ‘grids’ were performed during hydroacoustic krill surveys when blue whales were seen but not tagged. They were made between mid-May and the end of August in the EGSL (specifically in the SLE and the Gaspé Peninsula regions). Daytime vertical distributions for both krill species and for each survey are shown in Fig. S4. Generally, Arctic krill was located higher (50–110 m) in the water column than northern krill (100–150 m). Densities of Arctic krill were more uniformly distributed across depths than northern krill, which showed a spikier pattern (Fig. S4). Depth-specific mean densities of Arctic krill ranged from 4 to 50 g m^{-3} across surveys, with the 99th percentile reaching 4 to 250 g m^{-3} depending on the survey. Depth-specific mean densities of northern krill varied across a wider range of values among surveys, with densities varying from 4 to 76 g m^{-3} ; however, northern krill reached similar maximum densities as Arctic krill, with 99th percentiles varying from 4 to 260 g m^{-3} depending on the survey.

Among krill patches (4 g m^{-3} or above) detected during these 10 surveys, an average \pm SD of $11.7 \pm 13.0\%$ of those comprised of Arctic krill and $5.5 \pm 7.4\%$ of those comprised of northern krill contained bins (3 pings \times 0.5 m deep) that just met the densities required for a 25 m blue whale to achieve neutral energetic balance (FE = 1; Fig. 6). Only $1.7 \pm 2.5\%$ of Arctic krill patches and $2.1 \pm 3.4\%$ of northern krill patches allowed blue whales to forage with an efficiency of 2, and less than 1.5% allowed blue whales to reach FE \geq 3 (Fig. 6).

4. DISCUSSION

Prey density is the main driver of foraging effort, which together determine the FE at which an animal forages (MacArthur & Pianka 1966). For capital

Table 5. Trends in required density for Arctic and northern krill at various foraging efficiencies (FE = 1 to 4) with time of day based on generalized additive model results. N = 240 000 simulations for each model. Results (p-values) of the likelihood ratio test (LRT) for model selection against the null model (random effect only) are also presented. edf: estimated degrees of freedom

Response variable	Adjusted R ²	p	edf	F	LRT
Arctic krill density					
FE = 1	0.036	0.001	21.95	417.6	<0.0001
FE = 2	0.039	0.001	21.95	445.2	<0.0001
FE = 3	0.039	0.001	21.95	446.5	<0.0001
FE = 4	0.040	0.001	21.95	457.6	<0.0001
Northern krill density					
FE = 1	0.040	0.001	21.94	458.9	<0.0001
FE = 2	0.039	0.001	21.95	449.3	<0.0001
FE = 3	0.040	0.001	21.95	457.4	<0.0001
FE = 4	0.037	0.001	21.95	428	<0.0001

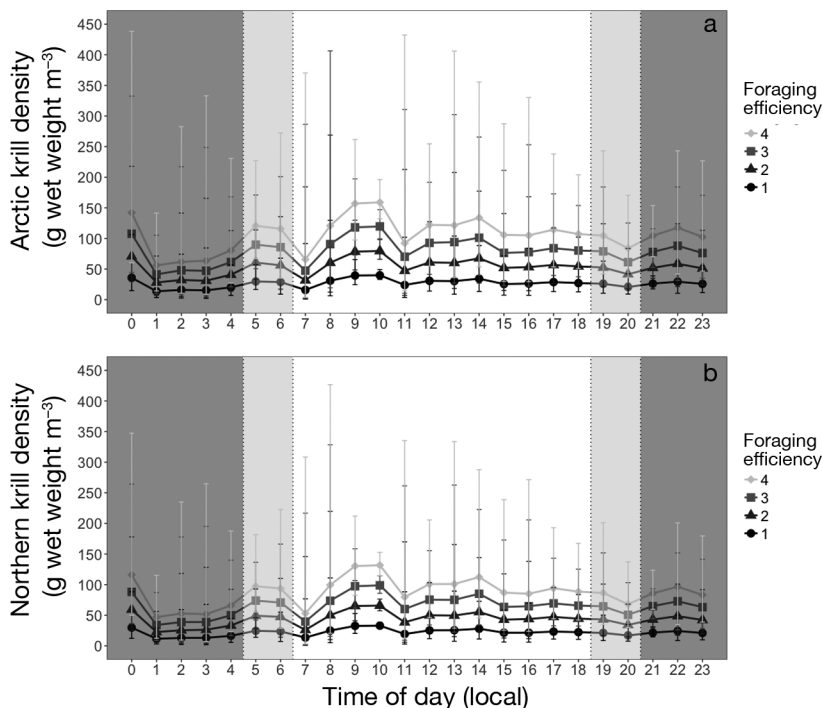


Fig. 5. Diel distribution of densities of (a) Arctic krill and (b) northern krill required by a 25 m blue whale feeding at foraging efficiencies varying from 1 to 4. Curves and bars represent the median and 90% confidence interval, respectively. Shaded areas are for nighttime (dark grey), dusk and dawn (light grey), and daytime (white)

breeders, maximizing FE allows maximizing energy storage to fuel survival, growth, and reproduction (Costa 1993). We used foraging effort inferred from biologging data and the resulting energy expenditures to estimate krill density requirements of blue whales foraging in the EGSL. Our study indicated that blue whales modulate their foraging effort throughout the day while maintaining stable energy expenditures. We estimated that during daytime, blue whales require minimum mean krill densities of 40.9 and 33.3 g m⁻³ depending on whether they feed on Arctic krill or northern krill. At night, they require lower mean densities of these 2 species to achieve this state, i.e. 31.7 and 25.8 g m⁻³, respectively. *In situ* measures of krill densities suggest that blue whales only sporadically find krill patches that allow for energy storage.

4.1. Hourly foraging effort and energy expenditure

The distribution of predators, and variations in their foraging effort throughout the day, likely reflect changes in the diel vertical distribution, density, and accessibility of their prey (Croll et al. 2005). For example, penguins adjust their residency time in a food patch according to their rate of energy gain (Watanabe et al. 2014), while krill-feeding humpback whales in Antarctica track the diel vertical migration of their prey and adjust their foraging effort accordingly (Friedlaender et al. 2016). In the latter study, humpback whales exhibited a higher number of lunges dive⁻¹ during daytime when feeding at depth than at night when feeding closer to the surface (Friedlaender et al. 2013, 2016), a similar pattern to what was observed in blue whales foraging in the SLE (Doniol-Valcroze et al. 2011, this study). Blue whales optimize FE by adjusting their foraging behavior according to vertical distributions and densities of krill (Hazen et al. 2015). In the northern Pacific Ocean, blue whales either feed close to the surface and breathe more often (thereby decreasing the risk of costly anaerobic metabolism as well as optimizing oxygen replenishment time) in low-density krill patches or increase their rate of energy gain in high-

Table 6. Standardized regression coefficients (SRC), minimum and maximum 95 % confidence intervals, biases and standard errors of the partial sensitivity analysis of the parameters used in Monte Carlo simulations. The largest contributors to the uncertainty in predicted krill density requirements are indicated in **bold**

Parameter	SRC	95 % CI		Bias	SE
		Min.	Max.		
Success rate	-0.002	-0.025	0.004	2.8×10^{-3}	0.010
Assimilation efficiency	-0.020	-0.038	-0.001	-8.6×10^{-5}	0.009
Krill energy content (kJ g ⁻¹ wet weight)	-0.103	-0.124	-0.081	-3.5×10^{-5}	0.011
Feeding rate (no. of lunges h ⁻¹)	-0.503	-0.520	-0.484	-5.5×10^{-4}	0.009
Energy expenditure (kJ)	0.480	0.463	0.499	3.8×10^{-4}	0.009
Volume engulfed (m ³)	0.002	-0.005	0.025	-2.2×10^{-3}	0.010

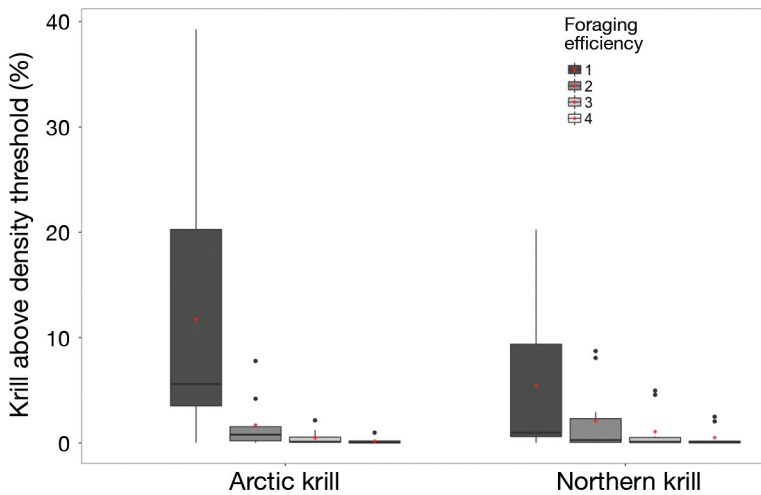


Fig. 6. Percentage of krill patches with 3-ping \times 0.5 m bins dense enough to allow blue whales to forage with efficiencies of 1 to 4 on Arctic krill and northern krill during daytime. Estimated krill density requirements (g wet weight m⁻³) were used as thresholds for foraging efficiencies of 1–4. For Arctic krill, mean estimates were 29, 57, 86, and 113 g m⁻³, respectively; for northern krill, these values were 24, 47, 70 and 94 g m⁻³, respectively. Means are represented by a red dot. Boxplots present the median (solid horizontal line), lower and upper quartiles (boxes), extreme values (whiskers) and outliers (points)

density krill patches by increasing the number of lunges dive⁻¹ (Hazen et al. 2015). Blue whales in the SLE follow a similar pattern and increase the number of lunges dive⁻¹ when feeding at increasingly deeper depths (Doniol-Valcroze et al. 2011).

Longer and deeper dives with several lunges are energetically more costly than shallower dives with a single mouthful (Acevedo-Gutiérrez et al. 2002, this study). Considering that hourly foraging effort exhibited by blue whales varied throughout the day, the associated hourly energy expenditure was expected to follow the same pattern. We had thus hypothesized that blue whale shallow feeding at night would reduce energy costs of transit, and result in lower hourly energy expenditures at that time of day. However, while significant diel variations were noted in

hourly foraging effort, overall the average energy expenditure remained stable throughout the day, leading us to reject our initial hypothesis. This relative stability in energy expenditure on an hourly basis was the result of the extra cost of diving deeper during daytime being counterbalanced by the combination of the increase in feeding rate at night and the high energetic cost of lunging. By modulating feeding rate (e.g. number of feeding dives h⁻¹ and number of lunges h⁻¹) and the number of lunges dive⁻¹ according to feeding depth, blue whales were able to achieve a nearly constant hourly energy expenditure. This means that blue whales can maximize net energy intake and FE by intensifying foraging when and where the energy return is expected to be the highest, i.e. at higher prey densities or shallower depths.

Unlike blue whales in the Pacific Ocean, which are known to feed at depths up to 250–300 m (Goldbogen et al. 2015, Hazen et al. 2015, Deruiter et al. 2017), blue whales in the SLE were not observed feeding at depths deeper than 100 m (Doniol-Valcroze et al. 2012) even though water depths can reach 300 to 500 m, depending on location. This indicates that blue whale foraging effort is likely driven by krill density, accessibility, and availability within that depth range. Krill vertical distribution data from hydroacoustic surveys in the EGSL show that the densest patches of the 2 studied krill species are generally located within the first 180 m of the water column during daytime (Plourde et al. 2014, McQuinn et al. 2015). Blue whales in the SLE also feed almost continuously (T. Doniol-Valcroze and V. Lesage unpubl. data); this is in contrast with krill-feeding humpback whales in Antarctica, which stop feeding in the morning when patches reach

their deepest depths (>100 m depth; Friedlaender et al. 2016). These differences in behavior among whale species may in part be related to size- and shape-specific metabolic considerations (Potvin et al. 2012). They may also arise from differences in krill densities among regions, with potentially lower krill densities in the St. Lawrence compared to Antarctica, possibly forcing a near-continuous feeding in the St. Lawrence in order for blue whales to accumulate fat reserves. Alternatively, it is possible that if krill also reach their deepest depths in the morning in the SLE, the perception of continuous feeding behavior arises from the small number of tags that were deployed early enough in the morning, or that lasted overnight to capture these early morning resting periods (V. Lesage unpubl. data).

Blue whales and other balaenopterids display a wide range of foraging strategies by modifying the kinematics of lunge feeding (e.g. speed, body orientation, inter-lunge intervals), in relation to prey density and the depth at which they feed to maximize prey intake and FE (Goldbogen et al. 2015, Cade et al. 2016). They perform more maneuvers when feeding on low-density and patchily distributed krill (Goldbogen et al. 2015). Also, the speed at which whales lunge likely affects energy expenditure since most of the cost arises from associated power and drag generated by a lunge (Goldbogen et al. 2012, Potvin et al. 2012, Potvin & Werth 2017). In this study, we could not account for the kinematics and maneuvering associated with feeding strategies due to the limited sensors available on our tags. Hence if whales lunge at lower speeds when feeding at shallow depths or on krill patches of lesser density, energy expenditure might be overestimated for these types of dives. The use of data loggers with supplementary sensors such as tri-axial accelerometers and magnetometers would provide more details about feeding maneuvering, and would help refine and improve the accuracy of energetic cost estimates related to foraging.

4.2. Krill density requirements

The sensitivity analyses revealed that the greatest uncertainty in our bioenergetics model output lay with the number of lunges h^{-1} , which was propagated to hourly energy expenditure. This parameter varied among individuals, possibly as a result of the heterogeneity of tag deployment duration and natural variation in blue whale activity budget and behavior. Increasing sample size might lower this uncer-

tainty. However, the high variability observed in the hourly foraging effort (number of feeding dives h^{-1} , number of lunges $\text{dive}^{-1} \text{h}^{-1}$, number of lunges h^{-1}) could also be ecologically relevant. Individuals of different sex, age, and reproductive status have different energetic requirements (Winship et al. 2002, Hammill et al. 2010, Fortune et al. 2013, Villegas-Amtmann et al. 2015) and are expected to display different behavioral patterns and foraging strategies (Hoskins & Arnould 2013, Hückstädt et al. 2018)

Krill density requirements were predicted based on the feeding rate (number of lunges h^{-1}), thus both are expected to be linked. For a given FE, whales required lower prey densities to meet the same energetic demands when performing more lunges (Figs. 1d,e, 4 & 5). In the morning when whales were observed diving deeper and for longer, krill density requirements were generally estimated to be higher. This is consistent with previous findings that fine-scale prey density, as opposed to prey biomass at a larger scale, is one of the most deterministic parameters in the foraging decision process when optimizing FE (Croll et al. 2005, Friedlaender et al. 2006). The minimum krill density thresholds required for a blue whale to achieve neutral balance was estimated at 14 to 40 g m^{-3} for Arctic krill and 11 to 33 g m^{-3} for northern krill, depending on time of day. This range of values encompasses the 12 g m^{-3} estimated by Hazen et al. (2015) off the Californian coast, where whale foraging behavior differs as a result of dense krill swarms occurring at deeper depths. This provides confidence in our model predictions. However, our estimate is lower than the mean density threshold below which blue whales reject swarms of krill in Antarctica, i.e. 110 g m^{-3} (range: 75–750) (Wiedenmann et al. 2011). In their study, Wiedenmann et al. (2011) fixed the number of lunges h^{-1} at 20, and limited feeding to daylight hours only. In our study, the number of daytime lunges was similar, but we allowed an additional 30 lunges per h^{-1} during nighttime foraging. These differences in model parameterization, where all capital needs to be accumulated during daytime in the Antarctic, led to a higher density threshold for profitability in Antarctic compared to St. Lawrence blue whales.

Prey densities required to fulfill energy demands are likely to vary with the targeted prey species and their energy content (Lockyer 2007). In our simulations, krill density requirements were slightly higher (22.8%) for Arctic krill than for northern krill, the latter of which have an energy content 21% higher than Arctic krill (5.2 ± 0.4 versus $4.3 \pm 0.6 \text{ g}^{-1}$, respectively). Arctic krill is also much smaller than northern

krill (mean length = 22.0 vs. 35.7 mm, respectively; McQuinn et al. 2013). The 2 krill species also differ in their aggregation behavior and 3-dimensional distribution (McQuinn et al. 2015). While the 2 species overlap in their vertical distributions, the center of mass of northern krill is typically found at depths 20–30 m deeper than that of Arctic krill (Plourde et al. 2014, McQuinn et al. 2015). Northern krill on average form looser aggregations ($<8 \text{ g m}^{-3}$) than Arctic krill ($8\text{--}16 \text{ g m}^{-3}$) and are generally found in lower-density patches than Arctic krill (McQuinn et al. 2015). Therefore, a blue whale would need to expend more energy finding sufficiently dense patches or would need to perform more lunges per dive when seeking northern krill than Arctic krill.

4.3. Coupling energetic requirements and *in situ* krill densities

The hydroacoustic krill surveys were performed as close in time and space as possible to observed but not tagged feeding blue whales, but it is unknown how long the whales had been feeding in the surveyed area. Therefore, the krill densities that were measured might not reflect exactly those that were available to blue whales at the time they started to feed, and may have decreased over time. We used the krill patches in areas where blue whales were observed as a sample of the type of patches blue whales are susceptible to exploit, and more specifically, to characterize the vertical distribution and densities of krill in these patches. We cannot exclude the possibility that denser patches occurred at locations where no blue whales were observed or at times when no hydroacoustic surveys were done. However, for the spatial aspect, the bias introduced in analysis of the availability of energetically suitable patches, if it exists, might be more toward an overrepresentation of higher-density patches than lower-density patches. Information currently available in the literature focuses on biomass density (g m^{-2}) rather than volumetric density (g m^{-3}) (e.g. Simard & Lavoie 1999, Sourisseau et al. 2006, McQuinn et al. 2015), preventing us from evaluating the size and direction of a potential bias. The hydroacoustic surveys were also conducted only during daytime and thus, could not capture prey density during nighttime, when both species migrate to the surface and form more diffuse patches (Berkes 1976, Simard et al. 1986). Obtaining accurate information at night might be challenging given that hydroacoustic measures can be negatively biased due to the blind zone of a

few meters below the echo sounders. Based on our hydroacoustic measurements, daytime krill densities that blue whales required to accumulate energy reserves were estimated to be scarce, suggesting that blue whales would need to seek the highest densities within krill patches to reach an FE above 2.

It is difficult to assess the FE value and period over which this FE needs to be maintained in order for free-ranging marine mammals to accumulate enough fat reserves to reproduce. Indications of adequate FE comes from 2 studies of income breeders (fur seals) showing an FE of 3.4 ± 0.4 on average in an increasing population (Antarctic fur seal) (Jeanniard-du-Dot et al. 2017b) and an FE of 2.2 ± 0.4 on average in a declining population (northern fur seal) (Jeanniard-du-Dot et al. 2018). In the declining population, ~45% of the studied individuals foraged at efficiencies close to or below 1 (Jeanniard-du-Dot et al. 2017b). In North Atlantic right whales, lipid reserves have been linked to reproductive performances, with pre-pregnant and pregnant females showing significantly thicker blubber than males or non-pregnant females (Miller et al. 2011). If energy stores are low, physiological mechanisms responsible for energy allocation prioritize processes involved in an animal's survival rather than reproduction (Bronson 1989, Schneider 2004). Our study indicates that blue whales in the EGSL may not often have the opportunity to forage at efficiencies higher than 2 and appear to have lower FE than other populations due to comparatively low krill densities. Observations of females with calves have been rare in this population, with fewer than 28 reports of cow-calf pairs over the past 35 yr (Mingan Island Cetacean Studies unpubl. data). Without further studies coupling blue whale feeding success and krill densities, and an extension of such studies to other areas where blue whales are known to occur in the western North Atlantic (Lesage et al. 2017), we can only speculate about a possible link between the low FEs predicted in our study and the low calving rate documented for this population (Mingan Island Cetacean Studies unpubl. data).

The EGSL, like several other marine systems in the world, is changing. Our study indicates that given the krill densities observed in this region, blue whales are more likely to achieve neutral energetic balance or accumulate body reserves by feeding on the highest available densities of Arctic krill than by feeding on the highest densities of northern krill. Currently, the krill biomass in the EGSL is dominated by Arctic krill, with a ratio between Arctic and northern krill of 60:40 (McQuinn et al. 2015). While *Thysanoessa inermis* also occurs in the EGSL and can be locally abun-

dant, this species has not been documented as a significant contributor to total krill biomass in this region (Berkes 1976). There are indications that blue whales in the EGSL tend to target Arctic krill preferentially (Gavrilchuk et al. 2014, McQuinn et al. 2016), and to forage within 100 m from the surface (Doniol-Valcroze et al. 2011, this study), a pattern consistent with the observed shallower mean center of mass for Arctic krill as compared to northern krill (McQuinn et al. 2015). However, northern krill can be more abundant than Arctic krill in some years (I. McQuinn unpubl. data); feeding on northern krill in these years would increase the energy expenditure associated with deeper diving. In other feeding areas of western North Atlantic blue whales, such as the Scotian Shelf, the krill species ratio is reversed, with northern krill forming the bulk of the krill biomass (Cochrane et al. 1991, 2000). Northern krill and Arctic krill differ in their thermal niche, with northern krill being a more temperate to boreal species and Arctic krill being better adapted to cold environments (Kulka et al. 1982, Simard et al. 1986, Plourde et al. 2014, McQuinn et al. 2015). With the prospect of a warming climate, the dominance ratio in the upper water column (above 100 m) between the 2 krill species is expected to change, which may affect blue whale spatial distribution and FE. Specifically, it would be of interest to examine the effects of changes in the ratio of Arctic krill biomass to northern krill biomass, absolute densities of the 2 species, and their vertical distribution on blue whale FE.

Our study was limited to the time of year that blue whales spend in the SLE in the summer, and thus we lack information about potential food sources they may find in other regions or at other times (Houston et al. 2007). We modeled energy requirements over 24 h to investigate fine-scale foraging behavior, recognizing that blue whales have an entire feeding season to meet their energy demands. Findings from this study could be taken one step further in future studies to incorporate stochastic changes in food availability or accessibility and examine how blue whales balance short-term potential deficits or benefits in FE over longer time periods. Consequently, extending our estimates of energy requirements to other seasons and over the geographic range of migrating blue whales would be useful to assess FE in other areas and at other times of the year relative to the availability and accessibility of resources. However, the amount of energy required during their migration, and to fuel the different annual life history stages, is difficult to estimate, especially for such large animals. Pirotta et al. (2018) developed a multi-annual bioenergetic model

for blue whales in the western North Pacific. It highlighted the complex interaction between a female's energy budget and her ability to reproduce, which requires detailed knowledge of behavioral, physiological, and environmental parameters. In the western North Atlantic, little is known about blue whale distribution and migration patterns outside the SLE and western GSL (but see Lesage et al. 2017). Quantifying their energy needs on a broader time scale, as well as estimating how far they can migrate and if reproduction is possible with the reserves they are accumulating, would be an essential next step.

In marine ecological studies, it is often logistically difficult to collect data on foraging effort and surrounding preyscape simultaneously. In this study, we used a reverse-engineering approach where preyscape and density requirements by a large marine predator were estimated from modeling energy expenditures derived from high-resolution diving behavior data. This approach offers an interesting perspective to conservation studies, as it provides a framework for estimating potential bioenergetic consequences of scenarios where anthropogenic activities or environmental factors might alter to various degrees the behavior of a predator or availability or quality of their prey.

Acknowledgements. We thank M. Moisan for tag conception; Y. Morin, J. Giard, D. Lefebvre, M. Moisan, R. Pintiaux, J. Winn, and S. Thompson for tag deployments; B. Woodward for providing access to the D-tag data; the Canadian Coast Guard crew aboard the 'Frederick G. Creed' and the various marine mammal observers for blue whale tracking and field support for the hydro-acoustic surveys; F. Paquet for help with the hydroacoustic data; A. Mosnier and P. Brosset for advice on the analysis; and the editor and the 3 anonymous reviewers for providing constructive comments which greatly improved the manuscript. This study was supported by the Species at Risk and Oceans Management programs of Fisheries and Oceans Canada, and by the strategic partnership grant (STPGP 447363) from the Natural Sciences and Engineering Research Council of Canada (NSERC) awarded to G.W. and V.L. This work contributes to the Québec-Océan program (a strategic cluster funded by the Fonds de Recherche du Québec—Nature et Technologies, FRQNT). J.A.G. was supported in part by a Terman Fellowship from Stanford University.

LITERATURE CITED

- ✦ Acevedo-Gutiérrez A, Croll DA, Tershy BR (2002) High feeding costs limit dive time in the largest whales. *J Exp Biol* 205:1747–1753
- ✦ Arnould JPY, Boyd IL, Speakman JR (1996) The relationship between foraging behaviour and energy expenditure in Antarctic fur seals. *J Zool (Lond)* 239:769–782
- ✦ Bailey H, Mate BR, Palacios DM, Irvine L, Bograd SJ, Costa DP (2009) Behavioural estimation of blue whale move-

- ments in the Northeast Pacific from state-space model analysis of satellite tracks. *Endang Species Res* 10: 93–106
- Beauchamp J, Bouchard H, de Margerie P, Otis N, Savaria JY (2009) Recovery strategy for the blue whale (*Balaenoptera musculus*), Northwest Atlantic population, in Canada. Species at Risk Act Recovery Strategy Series. Fisheries and Oceans Canada, Ottawa
- Berkes F (1976) Ecology of euphausiids in the Gulf of St. Lawrence. *J Fish Res Board Can* 33:1894–1905
- Boyd IL (1996) Temporal scales of foraging in a marine predator. *Ecology* 77:426–434
- Braithwaite JE, Meeuwig JJ, Letessier TB, Jenner KCS, Brierley AS (2015) From sea ice to blubber: linking whale condition to krill abundance using historical whaling records. *Polar Biol* 38:1195–1202
- Brodie P (1975) Cetacean energetics, an overview of intraspecific size variation. *Ecology* 56:152–161
- Bronson FH (1989) Mammalian reproductive biology. The University of Chicago Press, Chicago, IL
- Cabrol J, Trombetta T, Amaudrut S, Aulanier F and others (2019) Trophic niche partitioning of dominant North-Atlantic krill species, *Meganyctiphanes norvegica*, *Thysanoessa inermis*, and *T. raschii*. *Limnol Oceanogr* 64: 165–181
- Cade DE, Friedlaender AS, Calambokidis J, Goldbogen JA (2016) Kinematic diversity in orqual whale feeding mechanisms. *Curr Biol* 26:2617–2624
- Caraco T (1980) On foraging time allocation in a stochastic environment. *Ecology* 61:119–128
- Charnov EL (1976) Optimal foraging, the marginal value theorem. *Theor Popul Biol* 9:129–136
- Cochrane NA, Sameoto D, Herman AW, Neilson J (1991) Multiple-frequency acoustic backscattering and zooplankton aggregations in the inner Scotian Shelf basins. *Can J Fish Aquat Sci* 48:340–355
- Cochrane NA, Sameoto DD, Herman AW (2000) Scotian Shelf euphausiid and silver hake population changes during 1984–1996 measured by multi-frequency acoustics. *ICES J Mar Sci* 57:122–132
- Costa DP (1993) The relationship between reproductive and foraging energetics and the evolution of the Pinnipedia. *Symp Zool Soc Lond* 66:293–314
- Croll DA, Acevedo-Gutiérrez A, Tershy BR, Urbán-Ramírez J (2001) The diving behavior of blue and fin whales: Is dive duration shorter than expected based on oxygen stores? *Comp Biochem Physiol Part A Mol Integr Physiol* 129:797–809
- Croll DA, Marinovic B, Benson S, Chavez FP, Black N, Ternullo R, Tershy BR (2005) From wind to whales: trophic links in a coastal upwelling system. *Mar Ecol Prog Ser* 289:117–130
- Demer DA, Berger L, Bernasconi M, Bethke E and others (2015) Calibration of acoustic instruments. *ICES Coop Res Rep* 326. ICES, Copenhagen
- Deruiter SL, Langrock R, Skirbutas T, Goldbogen JA, Calambokidis J, Friedlaender AS, Southall BL (2017) A multivariate mixed hidden Markov model for blue whale behaviour and responses to sound exposure. *Ann Appl Stat* 11:362–392
- Doniol-Valcroze T, Lesage V, Giard J, Michaud R (2011) Optimal foraging theory predicts diving and feeding strategies of the largest marine predator. *Behav Ecol* 22: 880–888
- Doniol-Valcroze T, Lesage V, Giard J, Michaud R (2012) Challenges in marine mammal habitat modelling: evidence of multiple foraging habitats from the identification of feeding events in blue whales. *Endang Species Res* 17:255–268
- Emlen JM (1966) The role of time and energy in food preference. *Am Nat* 100:611–617
- Fahlman A, van der Hoop J, Moore MJ, Levine G, Rochon-Levine J, Brodsky M (2016) Estimating energetics in cetaceans from respiratory frequency: why we need to understand physiology. *Biol Open* 5:436–442
- Fortune SME, Trites AW, Mayo CA, Rosen DAS, Hamilton PK (2013) Energetic requirements of North Atlantic right whales and the implications for species recovery. *Mar Ecol Prog Ser* 478:253–272
- Friedlaender AS, Halpin PN, Qian SS, Lawson GL, Wiebe PH, Thiele D, Read AJ (2006) Whale distribution in relation to prey abundance and oceanographic processes in shelf waters of the Western Antarctic Peninsula. *Mar Ecol Prog Ser* 317:297–310
- Friedlaender AS, Tyson RB, Stimpert AK, Read AJ, Nowacek DP (2013) Extreme diel variation in the feeding behavior of humpback whales along the western Antarctic Peninsula during autumn. *Mar Ecol Prog Ser* 494: 281–289
- Friedlaender AS, Johnston DW, Tyson RB, Kaltenberg A and others (2016) Multiple-stage decisions in a marine central-place forager. *R Soc Open Sci* 3:160043
- Gavrilchuk K, Lesage V, Ramp C, Sears R, Bérubé M, Bearhop S, Beauplet G (2014) Trophic niche partitioning among sympatric baleen whale species following the collapse of groundfish stocks in the Northwest Atlantic. *Mar Ecol Prog Ser* 497:285–301
- Goldbogen JA, Calambokidis J, Shadwick RE, Oleson EM, McDonald MA, Hildebrand JA (2006) Kinematics of foraging dives and lunge-feeding in fin whales. *J Exp Biol* 209:1231–1244
- Goldbogen JA, Calambokidis J, Croll DA, Harvey JT and others (2008) Foraging behavior of humpback whales: kinematic and respiratory patterns suggest a high cost for a lunge. *J Exp Biol* 211:3712–3719
- Goldbogen JA, Potvin J, Shadwick R (2010) Skull and buccal cavity allometry increase mass-specific engulfment capacity in fin whales. *Proc R Soc B* 277:861–868
- Goldbogen JA, Calambokidis J, Oleson E, Potvin J, Pyenson ND, Schorr G, Shadwick RE (2011) Mechanics, hydrodynamics and energetics of blue whale lunge feeding: efficiency dependence on krill density. *J Exp Biol* 214: 131–146
- Goldbogen JA, Calambokidis J, Croll DA, McKenna MF and others (2012) Scaling of lunge-feeding performance in orqual whales: mass-specific energy expenditure increases with body size and progressively limits diving capacity. *Funct Ecol* 26:216–226
- Goldbogen JA, Calambokidis J, Friedlaender AS, Francis J and others (2013) Underwater acrobatics by the world's largest predator: 360° rolling manoeuvres by lunge-feeding blue whales. *Biol Lett* 9:20120986
- Goldbogen JA, Hazen EL, Friedlaender AS, Calambokidis J, Deruiter SL, Stimpert AK, Southall BL (2015) Prey density and distribution drive the three-dimensional foraging strategies of the largest filter feeder. *Funct Ecol* 29: 951–961
- Hammill MO, Ryg M, Chabot D (2010) Seasonal changes in energy requirements of harp seals. *J Northw Atl Fish Sci* 42:135–152

- Hazen EL, Friedlaender AS, Goldbogen JA (2015) Blue whales (*Balaenoptera musculus*) optimize foraging efficiency by balancing oxygen use and energy gain as a function of prey density. *Sci Adv* 1:e1500469
- Hoskins AJ, Arnould JPY (2013) Temporal allocation of foraging effort in female Australian fur seals (*Arctocephalus pusillus doriferus*). *PLOS ONE* 8:e79484
- Houston AI (1985) Central-place foraging: some aspects of prey choice for multiple-prey loaders. *Am Nat* 125: 811–826
- Houston AI, McNamara JM (1985) A general theory of central place foraging for single-prey loaders. *Theor Popul Biol* 28:233–262
- Houston AI, Stephens PA, Boyd IL, Harding KC, McNamara JM (2007) Capital or income breeding? A theoretical model of female reproductive strategies. *Behav Ecol* 18: 241–250
- Hückstädt LA, Holser RR, Tift MS, Costa DP (2018) The extra burden of motherhood: reduced dive duration associated with pregnancy status in a deep-diving mammal, the northern elephant seal. *Biol Lett* 14:20170722
- Jeanniard-du-Dot T, Trites AW, Arnould JPY, Speakman JR, Guinet C (2017a) Activity-specific metabolic rates for diving, transiting, and resting at sea can be estimated from time–activity budgets in ranging marine mammals. *Ecol Evol* 7:2969–2976
- Jeanniard-du-Dot T, Trites AW, Arnould JPY, Guinet C (2017b) Reproductive success is energetically linked to foraging efficiency in Antarctic fur seals. *PLOS ONE* 12: e0174001
- Jeanniard-du-Dot T, Trites AW, Arnould JPY, Speakman JR, Guinet C (2018) Trade-offs between foraging efficiency and pup feeding rate of lactating northern fur seals in a declining population. *Mar Ecol Prog Ser* 600:207–222
- Johnson MP, Tyack PL (2003) A digital acoustic recording tag for measuring the response of wild marine mammals to sound. *IEEE J Ocean Eng* 28:3–12
- Jonsson KI (1997) Capital and income breeding as alternative tactics of resource use in reproduction. *Oikos* 78: 57–66
- Kawamura A (1980) A review of food of balaenopterid whales. *Sci Rep Whales Res Inst* 32:155–197
- Kleiber M (1975) *The fire of life: an introduction to animal energetics*, 2nd edn. Robert E. Krieger, Huntington, NY
- Kulka DW, Corey S, Iles TD (1982) Community structure and biomass of euphausiids in the Bay of Fundy. *Can J Fish Aquat Sci* 39:326–334
- Lesage V, Gavrilchuk K, Andrews RD, Sears R (2017) Foraging areas, migratory movements and winter destinations of blue whales from the western North Atlantic. *Endang Species Res* 34:27–43
- Lockyer C (1981) Growth and energy budgets of large baleen whales from the Southern Hemisphere. *FAO Fish Ser* 5:379–487
- Lockyer C (2007) All creatures great and smaller: a study in cetacean life history energetics. *J Mar Biol Assoc UK* 87: 1035–1045
- MacArthur RH, Pianka ER (1966) On optimal land use of a patchy environment. *Am Nat* 100:603–609
- Madsen T, Shine R (1999) The adjustment of reproductive threshold to prey abundance in a capital breeder. *J Anim Ecol* 68:571–580
- Mårtensson PE, Nordøy ES, Blix AS (1994) Digestibility of krill (*Euphausia superba* and *Thysanoessa* sp.) in minke whales (*Balaenoptera acutorostrata*) and crabeater seals (*Lobodon carcinophagus*). *Br J Nutr* 72:713–716
- Mate BR, Lagerquist BA, Calambokidis J (1999) Movements of North Pacific blue whales during the feeding season off Southern California and their southern fall migration. *Mar Mamm Sci* 15:1246–1257
- McQuinn IH, Dion M, St. Pierre JF (2013) The acoustic multifrequency classification of two sympatric euphausiid species. *ICES J Mar Sci* 69:1205–1217
- McQuinn IH, Plourde S, St. Pierre JF, Dion M (2015) Spatial and temporal variations in the abundance, distribution, and aggregation of krill (*Thysanoessa raschii* and *Meganyctiphanes norvegica*) in the lower estuary and Gulf of St. Lawrence. *Prog Oceanogr* 131:159–176
- McQuinn IH, Gosselin JF, Bourassa MN, Mosnier A and others (2016) The spatial association of blue whales (*Balaenoptera musculus*) with krill patches (*Thysanoessa* spp. and *Meganyctiphanes norvegica*) in the estuary and northwestern Gulf of St. Lawrence. *Res Doc* 2016/104. DFO, Canadian Science Advisory Secretariat, Ottawa
- Miller CA, Reeb D, Best PB, Knowlton AR, Brown MW, Moore MJ (2011) Blubber thickness in right whales *Eubalaena glacialis* and *Eubalaena australis* related with reproduction, life history status and prey abundance. *Mar Ecol Prog Ser* 438:267–283
- Miller PJO, Biuw M, Watanabe YY, Thompson D, Fedak MA (2012) Sink fast and swim harder! Round-trip cost-of-transport for buoyant divers. *J Exp Biol* 215:3622–3630
- Narazaki T, Isojunno S, Nowacek DP, Swift R and others (2018) Body density of humpback whales (*Megaptera novaengliae* [sic]) in feeding aggregations estimated from hydrodynamic gliding performance. *PLOS ONE* 13: e0200287
- Olsen MA, Blix AS, Utsi TH, Sørmo W, Mathiesen SD (2000) Chitinolytic bacteria in the minke whale forestomach. *Can J Microbiol* 46:85–94
- Phillipson J (1964) A miniature bomb calorimeter for small biological samples. *Oikos* 15:130–139
- Piatt JF, Methven DA (1992) Threshold foraging behavior of baleen whales. *Mar Ecol Prog Ser* 84:205–210
- Pinheiro J, Bates D, DebRoy S, Sarkar D, R Core Team (2013) nlme: linear and nonlinear mixed effects models. R package version 3.1-131. <https://CRAN.R-project.org/package=nlme>
- Pirota E, Mangel M, Costa DP, Mate B and others (2018) A dynamic state model of migratory behavior and physiology to assess the consequences of environmental variation and anthropogenic disturbance on marine vertebrates. *Am Nat* 191:E40–E56
- Plourde S, McQuinn IH, Maps F, St-Pierre JF, Lavoie D, Joly P (2014) Daytime depth and thermal habitat of two sympatric krill species in response to surface salinity variability in the Gulf of St Lawrence, eastern Canada. *ICES J Mar Sci* 71:272–281
- Potvin J, Werth AJ (2017) Oral cavity hydrodynamics and drag production in balaenid whale suspension feeding. *PLOS ONE* 12:e0175220
- Potvin J, Goldbogen JA, Shadwick RE (2010) Scaling of lunge feeding in rorqual whales: an integrated model of engulfment duration. *J Theor Biol* 267:437–453
- Potvin J, Goldbogen JA, Shadwick RE (2012) Metabolic expenditures of lunge feeding rorquals across scale: implications for the evolution of filter feeding and the limits to maximum body size. *PLOS ONE* 7:e44854
- Pujol G, Iooss B, Janon A, Boumhaout K and others (2016) sensitivity: global sensitivity analysis of model outputs.

- R package version 1.12.1. <https://CRAN.R-project.org/package=sensitivity>
- Pyke G, Pulliam HR, Charnov EL (1977) Optimal foraging: a selective review of theory and tests. *Q Rev Biol* 52:137–154
- R Development Core Team (2017) R: a language and environment for statistical computing. R Foundation for Statistical Computing, Vienna
- Rosenberg DK, McKelvey KS (1999) Estimation of habitat selection for central-place foraging animals. *J Wildl Manag* 63:1028–1038
- Schneider JE (2004) Energy balance and reproduction. *Physiol Behav* 81:289–317
- Schoenherr JR (1991) Blue whales feeding on high concentrations of euphausiids around Monterey Submarine Canyon. *Can J Zool* 69:583–594
- Sears R, Calambokidis J (2002) Update COSEWIC status report on the blue whale *Balaenoptera musculus* in Canada. Committee on the Status of Endangered Wildlife in Canada, Ottawa
- Sears R, Perrin WF (2009) Blue whale (*Balaenoptera musculus*). In: Perrin WF, Würsig B, Thewissen JGM (eds) *Encyclopedia of marine mammals*. Academic Press, San Diego, CA, p 120–124
- Seyboth E, Groch KR, Dalla Rosa L, Reid K, Flores PAC, Secchi ER (2016) Southern right whale (*Eubalaena australis*) reproductive success is influenced by krill (*Euphausia superba*) density and climate. *Sci Rep* 6:28205
- Silva MA, Prieto R, Jonsen I, Baumgartner MF, Santos RS (2013) North Atlantic blue and fin whales suspend their spring migration to forage in middle latitudes: building up energy reserves for the journey? *PLOS ONE* 8:e76507
- Simard Y, Lavoie D (1999) The rich krill aggregation of the Saguenay—St. Lawrence Marine Park: hydroacoustic and geostatistical biomass estimates, structure, variability, and significance for whales. *Can J Fish Aquat Sci* 56:1182–1197
- Simard Y, Lacroix G, Legendre L (1986) Diel vertical migrations and nocturnal feeding of a dense coastal krill scattering layer (*Thysanoessa raschi* and *Meganyctiphanes norvegica*) in stratified surface waters. *Mar Biol* 91:93–105
- Sourisseau M, Simard Y, Saucier FJ (2006) Krill aggregation in the St. Lawrence system, and supply of krill to the whale feeding grounds in the estuary from the gulf. *Mar Ecol Prog Ser* 314:257–270
- Sparling CE, Georges JY, Gallon SL, Fedak M, Thompson D (2007) How long does a dive last? Foraging decisions by breath-hold divers in a patchy environment: a test of a simple model. *Anim Behav* 74:207–218
- Thompson D, Hiby AR, Fedak MA (1993) How fast should I swim? Behavioural implications of diving physiology. In: Boyd IL (ed) *Marine mammals: advances in behavioural and population biology*. Clarendon Press, Oxford, p 349–368
- Villegas-Amtmann S, Schwarz LK, Sumich JL, Costa DP (2015) A bioenergetics model to evaluate demographic consequences of disturbance in marine mammals applied to gray whales. *Ecosphere* 6:art183
- Ware C, Friedlaender AS, Nowacek DP (2011) Shallow and deep lunge feeding of humpback whales in fjords of the West Antarctic Peninsula. *Mar Mamm Sci* 27:587–605
- Ware C, Trites AW, Rosen DAS, Potvin J (2016) Averaged propulsive body acceleration (APBA) can be calculated from biologging tags that incorporate gyroscopes and accelerometers to estimate swimming speed, hydrodynamic drag and energy expenditure for Steller sea lions. *PLOS ONE* 11:e0157326
- Watanabe YY, Ito M, Takahashi A (2014) Testing optimal foraging theory in a penguin–krill system. *Proc R Soc B* 281:20132376
- Watkins JL, Murray AWA (1998) Layers of Antarctic krill, *Euphausia superba*: Are they just long krill swarms? *Mar Biol* 131:237–247
- Wheatley KE, Bradshaw CJA, Harcourt RG, Hindell MA (2008) Feast or famine: evidence for mixed capital-income breeding strategies in Weddell seals. *Oecologia* 155:11–20
- Wiedenmann J, Cresswell KA, Goldbogen JA, Potvin J, Mangel M (2011) Exploring the effects of reductions in krill biomass in the Southern Ocean on blue whales using a state-dependent foraging model. *Ecol Model* 222:3366–3379
- Williams TM, Davis RW, Fuiman LA, Francis J and others (2000) Sink or swim: strategies for cost-efficient diving by marine mammals. *Science* 288:133–136
- Winship AJ, Trites AW, Rosen DAS (2002) A bioenergetic model for estimating the food requirements of Steller sea lions *Eumetopias jubatus* in Alaska, USA. *Mar Ecol Prog Ser* 229:291–312
- Wood S (2006) Mixed GAM computation vehicle with automatic smoothness estimation. R package version 1.8-17. <https://CRAN.R-project.org/package=mgcv>

Editorial responsibility: Peter Corkeron,
Woods Hole, MA, USA

Submitted: February 14, 2019; Accepted: June 27, 2019
Proofs received from author(s): August 18, 2019